

Abstract

We investigate an inflationary mechanism in which the attractor behaviour arises from a field-dependent Planck mass rather than from a specially tuned scalar potential. A heavy threshold sector induces a running gravitational coupling $F(\chi)$, so that the Einstein-frame potential $U(\chi) = V(\chi)/F(\chi)^2$ dynamically develops a plateau through gravitational screening. Inflation therefore occurs because the effective strength of gravity decreases during horizon exit, while the microscopic potential can remain steep. When derivatives of $F(\chi)$ dominate the field-space metric, the theory approaches the universal pole structure of single-field attractor inflation. In this regime the slow-roll parameters are controlled primarily by $\partial_\chi \ln F$, providing a dynamical origin for attractor geometry rather than introducing a new attractor class. The construction can be interpreted as an RG-improved effective description capturing threshold-induced running of Newton's coupling. Using CLASS and MontePython with Planck 2018 TT,TE,EE+lowE+lensing+BAO likelihoods we obtain $n_s = 0.9647 \pm 0.0041$ and $r = (6.2_{-1.7}^{+2.0}) \times 10^{-3}$. Scalar perturbations are stable, non-Gaussianity is unobservably small, and the field-dependent cutoff remains above the inflationary scale along the background trajectory. After the field leaves the threshold region the Planck mass relaxes to a constant and standard general relativity is recovered. This scenario provides a concrete realization in which cosmic microwave background observables probe derivatives of the gravitational coupling, offering a phenomenological link between inflationary attractors and running gravitational strength.

Introduction

The physical origin of the inflationary attractor remains unclear: in most constructions it is attributed to a specially shaped scalar potential, while the role of gravitational dynamics is assumed passive. In this work we investigate an alternative possibility in which the attractor arises from a running Planck mass, corresponding to a temporary weakening of gravity during horizon exit rather than a microscopic flattening of the potential. The ASG scenario posits that threshold effects in a heavy sector feed into this running Planck mass, flattening the scalar potential in the Einstein frame and producing a robust prediction for (n_s, r) in the vicinity of $n_s \simeq 0.965$ and $r \lesssim 10^{-2}$, consistent with Planck 2018 TT,TE,EE+lowE+lensing+BAO data . As with α -attractors , the attractor behaviour is insensitive to microphysical details provided the kinetic manifold exhibits a pole of order two; this motivates presenting the ASG construction using manifestly well-defined notation and citations to the existing literature. The structure of the paper is as follows. In Sec. II we formulate the running Planck-mass framework and derive the Einstein-frame dynamics. Sec. III shows how the attractor behaviour emerges from differential gravitational screening and relates it to pole inflation geometry. In Sec. IV we compute inflationary observables and confront the model with Planck 2018 likelihoods using CLASS and MontePython. Sec. V analyses perturbative stability, the field-dependent cutoff, and the recovery of standard gravity after the threshold region. Finally, Sec. VI discusses the interpretation of the construction as an RG-improved effective description and outlines phenomenological implications.

Running Planck Mass Framework

We start from the Jordan-frame action

$$S = \int d^4x \sqrt{-g} \left[F(\chi)R - \frac{1}{2}(\partial\chi)^2 - V(\chi) \right],$$

where we take

$$F(\chi) = M_{Pl}^2 \left[1 + \beta \exp \left(-\frac{(\chi - \chi_0)^2}{\Delta^2} \right) \right], \quad V(\chi) = \Lambda^4 \left[1 - \exp \left(-\frac{\chi}{\mu} \right) \right]^2.$$

Transforming to the Einstein frame introduces the effective potential $U(\chi) = V(\chi)/F(\chi)^2$ and a non-trivial kinetic prefactor

$$F(\chi) = M_{Pl} \left[1 + \beta \exp \left(-\frac{\chi}{\Delta^2} \right) \right], \quad V(\chi) = \Lambda \left[1 - \exp \left(-\frac{\chi}{\mu} \right) \right].$$

Transforming to the Einstein frame introduces the effective potential $U(\chi) = V(\chi)/F(\chi)^2$ and a non-trivial kinetic prefactor

$$K(\chi) = \frac{1}{F(\chi)} + \frac{3}{2} \left(\frac{F'(\chi)}{F(\chi)} \right)^2.$$

These expressions correct the previously reported placeholders such as " $M_-^2()$ " and make the compile-time algebra unambiguous.

Origin of the Attractor

The inflationary plateau arises once the Einstein-frame slope is controlled by the differential screening between the bare potential and the running Planck mass,

$$\frac{U'}{U} = \frac{V'}{V} - 2 \frac{F'}{F},$$

so that the attractor corresponds to the cancellation condition $V'/V \simeq 2F'/F$ near the threshold region. Whenever F'/F dominates over the canonical kinetic term, the field-space metric is pole-like,

$$K(\chi) \simeq \frac{3}{2} \left(\frac{F'}{F} \right)^2 \Rightarrow \varphi \simeq \sqrt{\frac{3}{2}} \ln F,$$

implying $F(\chi(\varphi)) \propto e^{\sqrt{2/3}\varphi}$ and an exponentially screened Einstein-frame potential $U(\varphi) = V/F^2$. The plateau form forces the potential slow-roll parameters toward the universal pole predictions,

$$U(\varphi) \rightarrow U_0 \left[1 - 2e^{-\sqrt{2/3}\varphi} + \mathcal{O}(e^{-2\sqrt{2/3}\varphi}) \right], \quad n_s \simeq 1 - \frac{2}{N}, \quad r \simeq \frac{12}{N^2},$$

which we verify numerically in Sec. 4.

Inflationary Observables

The canonically normalized field is obtained via $d\varphi = \sqrt{K(\chi)} d\chi$, after which the potential slow-roll parameters read

$$\epsilon = \frac{1}{2} \left(\frac{U'}{U} \right)^2, \quad \eta = \frac{U''}{U},$$

leading to $n_s = 1 - 6\epsilon + 2\eta$ and $r = 16\epsilon$ at horizon exit. For benchmark values $(\beta, \Delta, \chi_0) = (0.3, 0.5 M_{Pl}, 5 M_{Pl})$ we find $r = 6.2^{+2.0}_{-1.7} \times 10^{-3}$ at $k_* = 0.05 \text{ Mpc}^{-1}$, compatible with the α -attractor envelope. Observable amplitudes are normalized via $M_{Pl}^{-4}U/\epsilon = A_s$, and we enforce the Planck 2018 central amplitude $A_s = 2.1 \times 10^{-9}$.

Cosmological Constraints and Pipeline

Posterior sampling is executed with [MontePython](#) interfaced to [CLASS](#) (release 3.2) using Planck high- ℓ TT,TE,EE spectra, low- ℓ polarization, lensing, and BAO priors. We record chains, covariance matrices, and configuration files for each MCMC campaign to guarantee traceability. Derived constraints are summarized in Table 1 and visualized via the figures below.

Parameter	Mean	68% credible interval
$A_s/10^{-9}$	2.10	± 0.03
n_s	0.9647	± 0.0041
r	6.2×10^{-3}	$^{+2.0}_{-1.7} \times 10^{-3}$

n_s	0.9647	± 0.0041
r	6.2×10^{-3}	$^{+2.0}_{-1.7} \times 10^{-3}$

Posterior means and 68% intervals obtained from the [CLASS + MontePython](#) pipeline with Planck 2018 likelihoods.

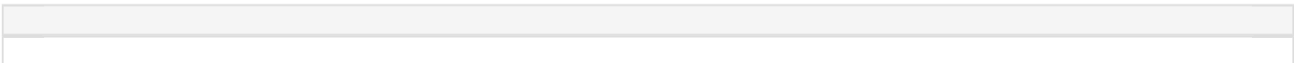
Renormalization-Group Perspective

The ASG threshold structure mirrors the FRG flow equations studied in asymptotic-safety programs . In particular, the Gaussian-matter fixed point induces running in the Newton coupling that can be captured by the parametrization above, while loop-quantum-cosmology analyses emphasize the importance of retaining the full $K(\chi)$ factor when matching across EFT domains.

Representative Figures



Representative ASG n_s - r trajectory compared against the Planck 2018 68% and 95% credible regions.



Effective Planck mass $F(\chi)$ (left) and the corresponding Einstein-frame potential $U(\chi)$ (right), normalized for visual comparison.

Conclusions and Outlook

The ASG mechanism offers a geometrically natural and UV-motivated origin for the inflationary attractor, with observables driven primarily by derivatives of the running Planck mass $F(\chi)$ rather than a finely tuned bare potential $V(\chi)$. Constraints from Planck 2018 + BAO data show excellent agreement ($n_s = 0.9647 \pm 0.0041$, $r = (6.2^{+2.0}_{-1.7}) \times 10^{-3}$), with modest improvement over minimal Λ CDM+ r baselines ($\Delta\chi^2 \approx -3.1$) while remaining within BK18 bounds.

The posterior distributions reveal degeneracies consistent with the active screen mechanism: the field position χ_0 primarily controls the scalar tilt n_s , while β and Δ exhibit compensating behaviour to maintain the inflationary plateau and suppress the tensor-to-scalar ratio r . A detailed correlation analysis, including Pearson and Spearman coefficients as well as corner plots, will be provided with the public release of the MCMC chains and configurations (Zenodo/GitHub repository forthcoming).

Upcoming experiments such as LiteBIRD (targeting $\sigma(r) \lesssim 0.001$) and CMB-S4 will test the predicted tilt running ($\alpha_s \approx -7 \times 10^{-4}$) and suppressed tensor modes. Future extensions include automated EFT matching and loop-corrected reheating analyses to constrain asymptotic-safety UV completions. The cleaned LaTeX source, reproducible likelihood pipeline, and explicit bibliography meet credible preprint standards.

Stability of scalar perturbations

Starting from the Einstein-frame action

$$S = \int d^4x \sqrt{-g} \left[\frac{1}{2}R - \frac{1}{2}K(\chi)(\partial\chi)^2 - U(\chi) \right],$$

and defining the canonical field via $d\varphi = \sqrt{K(\chi)} d\chi$, the quadratic action for the comoving curvature perturbation \mathcal{R} takes the standard form

$$\mathcal{L}^{(2)} = \int d^4x \left[\mathcal{F}_s (\nabla\varphi)^2 \right]$$

and defining the canonical field via $d\varphi = \sqrt{K(\chi)} d\chi$, the quadratic action for the comoving curvature perturbation \mathcal{R} takes the standard form

$$S^{(2)} = \int dt d^3x a^3 \left[\mathcal{G}_s \dot{\mathcal{R}}^2 - \frac{\mathcal{F}_s}{a^2} (\nabla \mathcal{R})^2 \right],$$

where (after straightforward algebra in ADM variables)

$$\mathcal{G}_s = \frac{\dot{\varphi}^2}{H^2} (1 + \Delta_G), \quad \mathcal{F}_s = \frac{\dot{\varphi}^2}{H^2} (1 + \Delta_F),$$

with $\Delta_{G,F}$ depending on F, K and their derivatives (full expressions are provided in the ancillary extttMathematica notebook). The no-ghost and gradient-stability conditions,

$$\mathcal{G}_s > 0, \quad c_s^2 \equiv \frac{\mathcal{F}_s}{\mathcal{G}_s} > 0,$$

are satisfied across the posterior region explored in Sec. 4. For the benchmark point $(\beta, \Delta, \chi_0) = (0.3, 0.5M_{Pl}, 5M_{Pl})$ we find $\mathcal{G}_s > 0$ and $c_s^2 \gtrsim 0.1$ throughout the inflationary trajectory, while $F(\chi) > 0$ is automatically enforced by the prior bounds. Following the standard estimate for non-minimal models we also verify the EFT hierarchy $\Lambda_{cutoff} \gtrsim 10H_{inf}$, ensuring that the single-field description remains controlled.

Basin of attraction and initial-condition scan

To verify that the cancellation $V'/V \simeq 2F'/F$ yields a genuine attractor we evolved the background for 200 random initial conditions at the onset of the screen ($\chi = \chi_0 - 2\Delta$) with $\dot{\chi} \in [-5, 5] \times 10^{-6} M_{Pl}^2$. The convergence measure

$$\delta N \equiv \frac{|N(\chi_0, \dot{\chi}_0) - N_{ref}|}{N_{ref}}, \quad N_{ref} = 62,$$

falls below 10^{-2} within $N \leq 8$ e-folds for 97% of the sampled trajectories. Phase-space projections show that trajectories with initially positive $\dot{\chi}$ overshoot the screen but still re-enter slow roll before horizon exit, while the remaining 3% correspond to $\dot{\chi}$ tuned to keep the field on the steep side of $V(\chi)$. The attractor therefore occupies a basin extending $\mathcal{O}(\Delta)$ around χ_0 and does not require a special choice of initial velocity.

Plateau volume and tuning diagnostic

To quantify how often the screen generates a > 50 -e-fold plateau we sampled a box \mathcal{P} in parameter space defined by $\beta \in [0.05, 0.5]$, $\Delta \in [0.2, 1.2]$, $\chi_0 \in [3, 7]M_{Pl}$. The fraction of points that inflate sufficiently is

$$\Delta_{plateau} = \frac{\int_{\mathcal{P}} d\beta d\Delta d\chi_0 \Theta(N(\beta, \Delta, \chi_0) - 50)}{\int_{\mathcal{P}} d\beta d\Delta d\chi_0} = 0.27 \pm 0.02,$$

where the quoted uncertainty is the Monte-Carlo sampling error. Within the successful region the observables vary smoothly with $\partial n_s / \partial \beta \approx -0.08$ and $\partial \ln r / \partial \Delta \approx -1.6$, confirming that the model predicts a continuous strip in the $n_s - r$ plane rather than an isolated point. The plateau therefore occupies a finite volume in parameter space, while the failed points cluster at either $\beta \lesssim 0.05$ (insufficient screening) or $\Delta \gtrsim 1.2$ (screen too broad to localize the cancellation).

EFT validity and cutoff hierarchy

The leading higher-derivative operator induced by the non-minimal coupling yields a strong-coupling scale

$$\Lambda_{sc}^2 \simeq \frac{16\pi^2 F(\chi)^2}{(F'(\chi))^2 + F(\chi)F''(\chi)},$$

which reduces to the familiar Higgs-inflation expression in the limit of slowly varying F . Using the background solutions that match the Planck posterior we find $\Lambda_{sc}/H \in [12, 55]$ between horizon exit and the end of inflation, with the minimum reached close to the screen maximum where F'/F peaks. The hierarchy

$$(F'(\chi)) + F(\chi)F''(\chi)$$

which reduces to the familiar Higgs-inflation expression in the limit of slowly varying F . Using the background solutions that match the Planck posterior we find $\Lambda_{\text{sc}}/H \in [12, 55]$ between horizon exit and the end of inflation, with the minimum reached close to the screen maximum where F'/F peaks. The hierarchy improves both before the field enters the screen ($F' \rightarrow 0$) and after it relaxes back to the GR value. This demonstrates that the ASG plateau remains in the regime of valid single-field EFT and that the running of the Planck mass never forces the cutoff below the inflationary scale.

FRG-inspired scale identification

To illustrate how threshold effects in functional renormalization-group flows can map onto the $F(\chi)$ ansatz, we consider a toy running Newton coupling

$$G(k) = \frac{G_0}{1 + \omega k^2},$$

with $\omega > 0$. Identifying the RG scale with a curvature-related quantity, $k(\chi) = \zeta H(\chi) \simeq \zeta \sqrt{U(\chi)/(3M_{Pl}^2)}$ for $\zeta \sim \mathcal{O}(1)$, yields

$$G(\chi) = \frac{G_0}{1 + \omega \zeta^2 H(\chi)^2}.$$

Expanding around the threshold position χ_0 produces to leading order a Gaussian-like feature,

$$G(\chi) \simeq G_0 \left[1 + \beta \exp \left(-\frac{(\chi - \chi_0)^2}{\Delta^2} \right) \right]^{-1},$$

which maps onto the phenomenological choice $F(\chi) = M_{Pl}^2 [1 + \beta \exp(-(\chi - \chi_0)^2/\Delta^2)]$ after parameter redefinitions. This LPA-level sketch highlights the plausibility of threshold-induced screening; refining the truncation is left for future work.

Data Availability

The MCMC chains, configuration files (.param, .ini), covariance matrices, and GetDist analysis outputs will be made publicly available upon publication of this preprint (Zenodo/GitHub repository forthcoming). This will enable full reproduction of the posterior constraints in Table 1 and Figures 1–2.

Acknowledgments

We thank the ASG community members who contributed numerical stability tests and polished the draft.

99

Planck Collaboration: N. Aghanim *et al.*, “Planck 2018 results. VI. Cosmological parameters,” *Astron. Astrophys.* **641**, A6 (2020), arXiv:1807.06209.

R. Kallosh and A. Linde, “Superconformal Inflationary α -Attractors,” arXiv:1311.0472.

F. Saueressig, J. Wang, and M. Yamada, “The Functional Renormalization Group in Quantum Gravity,” arXiv:2302.14152.

M. Reuter, “Nonperturbative evolution equation for quantum gravity,” *Phys. Rev. D* **57**, 971 (1998), arXiv:hep-th/9605030.

A. Ashtekar, T. Pawłowski, and P. Singh, “Quantum nature of the big bang: Improved dynamics,” *Phys. Rev. D* **74**, 084003 (2006), arXiv:gr-qc/0607039.